

Convergence of Unilateral Laplace Transforms on Time Scales

John M. Davis · Ian A. Gravagne ·
Robert J. Marks II

Received: 22 May 2009 / Revised: 29 September 2009
© Springer Science+Business Media, LLC 2010

Abstract A time scale is any closed subset of the real line. Continuous time and discrete time are special cases. The unilateral Laplace transform of a signal on a time scale subsumes the continuous-time unilateral Laplace transform, and the discrete-time unilateral z -transform as special cases. The regions of convergence (ROCs) time scale Laplace transforms are determined by the time scale's graininess. For signals with finite area, the ROC for the Laplace transform resides outside of a Hilger circle determined by the time scales's smallest graininess. For transcendental functions associated with the solution of linear time-invariant differential equations, the ROCs are determined by function parameters (e.g., sinusoid frequency) and the largest and smallest graininess values in the time scale. Since graininess always lies between zero and infinity, there are ROCs applicable to a specified signal on any time scale. All ROCs reduce to the familiar half-plane ROCs encountered in the continuous-time unilateral Laplace transform and circle ROCs for the unilateral z -transform. If a time scale unilateral Laplace transform converges at some point in the transform plane, a region of additional points can be identified as also belonging to the larger ROC.

Keywords Time scales · Laplace transform · z -transforms · Region of convergence · Hilger circle

This work was supported by National Science Foundation grant CMMI #0726996.

J.M. Davis
Department of Mathematics, Baylor University, One Bear Place #97328, Waco, TX 76798-7328,
USA
e-mail: John_M_Davis@Baylor.edu

I.A. Gravagne · R.J. Marks II (✉)
Department of Electrical and Computer Engineering, Baylor University, One Bear Place #97356,
Waco, TX 76798-7356, USA
e-mail: Robert_Marks@baylor.edu

I.A. Gravagne
e-mail: Ian_Gravagne@Baylor.edu

1 Introduction

A time scale is any closed subset of the real line. Continuous time, \mathbb{R} , and discrete time, \mathbb{Z} , are special cases. The calculus of time scales was introduced by Hilger [8]. Time scales have found utility in describing the behavior of dynamic systems [1, 10] and have been applied to control theory [3, 4, 6].

Laplace transformation of signals on time scales was first considered by Hilger [9]. The development of unilateral Laplace transforms on time scales, however, is due to Bohner and Peterson [1]. The conventional continuous-time Laplace transform and discrete-time z -transform are special cases.

Bohner and Peterson's development, however, did not address regions of convergence (ROCs) in the transform domain. Some initial work in this area was done by our group [5]. In this paper, we complete this work by presenting the ROCs of the transcendental functions arising from the solution of linear time-invariant dynamic equations on time scales [1]. There are three cases of time scales considered.

1. Time scales whose graininess is bounded from above and below
 - over the entire time scale, or
 - in an asymptotic sense.
2. Time scales whose asymptotic graininess approaches a constant. \mathbb{R} and \mathbb{Z} are special cases. All time scales in this class are also asymptotically a member of the time scales in 1).
3. All time scales. This can be considered a limiting special case of 1) since the graininess of any time scales is bounded between zero and infinity.

The unilateral Laplace transform on time scales proves fundamental for signal processing on time scales, including signal filtering, convolution, and the modeling stochastic of processes [5, 11–13].

2 Time Scales

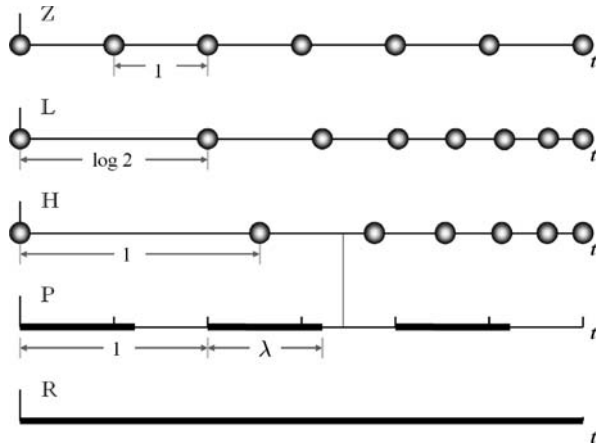
Our review of time scales contains only material germane to unilateral Laplace transforms. The text by Bohner and Peterson [1] contains a complete introduction to the topic. There is also a tutorial available online.¹

A time scale, \mathbb{T} , is any collection of closed sets of points on the real time axis. Continuous time, \mathbb{R} , and discrete time, \mathbb{Z} , are special cases. Some useful time scale types include

- *Causal time scales*, \mathbb{T}^+ , containing only points for nonnegative values of time.
- A *discrete time scale*, \mathbb{D} , containing only isolated points.

¹TimeScales.org.

Fig. 1 Some time scales. Discrete time is \mathbb{Z} and continuous time is \mathbb{R}



Some examples of time scales, illustrated in Fig. 1, include

- *Discrete time*, \mathbb{Z} .
- *Causal discrete time*, which contains all nonnegative integers and is depicted by \mathbb{Z}^+ .
- The *log time scale*, also discrete and causal, is

$$\mathbb{L}^+ = \{t \mid t = \log n, n \in \mathbb{N}\}.$$

The base of the log is a parameter of the time scale. The log time scale is discrete and causal.

- The *harmonic time scale*, $\mathbb{H}^+ = \{t_n \mid t_0 = 0, t_n = \mathcal{H}_n \text{ for } n \in \mathbb{N}\}$ where the n th harmonic number is

$$\mathcal{H}_n = \sum_{k=1}^n \frac{1}{k}.$$

The harmonic time scale is both discrete and causal.

- A *periodic piecewise continuous time scale* with duty cycle $\lambda < 1$ is the set of points

$$\mathbb{P} = \{t \mid t \in [n, n + \lambda], n \in \mathbb{Z}\}.$$

- A causal discrete *periodic time scale* has an initial period of N points, $\mathbb{S} = \{t_0, t_1, \dots, t_N\}$. For a positive constant, T , the time scale is then

$$\mathbb{B} = \{t = t_n + mT, t_n \in \mathbb{S}, m \in \mathbb{Z}^+\}.$$

- The causal and discrete *quantum time scale*, \mathbb{Q} , is parameterized by the positive number $q > 1$,

$$\mathbb{Q} = \{t \mid t = 0, t = q^n, n \in \mathbb{Z}^+\},$$

where \mathbb{Z}^+ is the set of all nonnegative integers.

- A *stochastic time scale*, such as a Poisson process [12], is a discrete time scale whose points are randomly chosen.
- The *continuous time scale* is denoted by an \mathbb{R} .
- The *causal continuous time scale* contains all nonnegative values of t and is depicted by \mathbb{R}^+ .

A time scale $h\mathbb{T}$ denotes a time scale where each $t \in \mathbb{T}$ is replaced by ht . Thus, for example,

$$h\mathbb{P} = \{t \mid t \in [hn, h(n + \lambda)], n \in \mathbb{Z}\}$$

repeats periodically with period h .

2.1 The Forward Jump Operator and Time Scale Graininess

For a time scale, \mathbb{T} , at a given time, t , the subsequent element in the time scale is denoted by the *forward jump operator*,

$$\sigma(t) := \inf_{\tau > t, \tau \in \mathbb{T}} \tau. \quad (2.1)$$

We will also use the notation t^σ to characterize this point. The distance between t and its next point is called the *graininess* of the time scale and is written

$$\mu(t) := \sigma(t) - t.$$

The graininess is nonnegative

$$0 \leq \mu(t) < \infty. \quad (2.2)$$

Here are some examples.

- On \mathbb{Z} , when $t = n$, we have $\sigma(t) = n + 1$ and $\mu(t) = 1$.
- On \mathbb{R} , we have $\sigma(t) = t + dt$ and $\mu(t) = dt$. Rigorously, then, $\mu(t) = 0$.
- On the log time scale, $\sigma(t) = \log(n + 1)$ and $\mu(t) = \log(1 + \frac{1}{n})$.
- For the harmonic time scale, $\sigma(t) = \mathcal{H}_{n+1}$ and $\mu(t) = \frac{1}{n+1}$.
- For the periodic time scale, \mathbb{P} ,

$$\mu(t) = \begin{cases} dt; & t \in [n, n + \lambda), \\ 1 - \lambda; & t = n + \lambda. \end{cases}$$

2.2 Differentiation and Integration on Time Scales

The Hilger derivative of a signal $f(t)$ defined on a time scale \mathbb{T} is defined by

$$f^\Delta(t) = \frac{f(t^\sigma) - f(t)}{\mu(t)}. \quad (2.3)$$

Note that, as a special case, the Hilger derivative on \mathbb{Z} is the forward difference. Since $t = n$, $f^\Delta(n) = \Delta f(n) = f(n + 1) - f(n)$. For \mathbb{R} (and on continuous intervals), (2.3) is interpreted in the limiting sense and $f^\Delta(t) = \frac{df(t)}{dt}$.

Hilger integration is most easily introduced by the antiderivative. A more rigorous treatment is given in Bohner and Peterson [2]. Guseinov [7] provides a measure theoretic [14] treatment of time scale integration.

Let $g(t) = f^\Delta(t)$. Then, for $(a, b) \in \mathbb{T}$,

$$f(t) = \int_0^t g(\tau) \Delta \tau + \text{constant}.$$

The definite integral follows as

$$\int_a^b g(\tau) \Delta \tau = f(b) - f(a).$$

2.3 Time Scale Exponentials

For the dynamic time scale differential equation

$$f^\Delta(t) = p(t) f(t)$$

the solution, for the initial condition $f(0) = 1$, is $f(t) = e_{p(t)}(t)$, where

$$e_{p(t)}(t) := \exp\left(\int_{\tau=0}^t \frac{\log_e(1 + \mu(\tau)p(\tau))}{\mu(\tau)} \Delta \tau\right). \tag{2.4}$$

When $p(t)$ is set to a constant, p , we obtain the following special cases.

- On \mathbb{R} , we obtain the familiar result

$$e_p(t) = e^{pt}.$$

- On a discrete time scale, \mathbb{D} ,

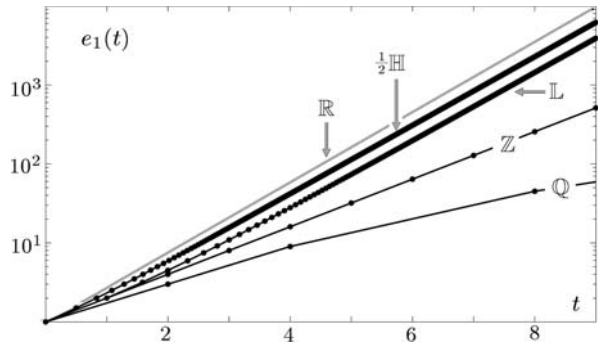
$$e_p(t_n) = \begin{cases} \prod_{k=0}^{n-1} (1 + \mu(t_k)p); & n > 0, \\ 1; & n = 0, \\ \prod_{k=n}^{-1} (1 + \mu(t_k)p)^{-1}; & n < 0. \end{cases} \tag{2.5}$$

- On \mathbb{Z} , it follows from (2.5) that

$$e_p(t_n) = \begin{cases} (1 + p)^n; & n > 0, \\ 1; & n = 0, \\ (1 + p)^{-n}; & n < 0. \end{cases}$$

Plots of $e_1(t)$ for some time scales are shown in Fig. 2.

Fig. 2 Plots of $e_1(t)$ for $t \geq 0$ for the time scales $\mathbb{R}, \mathbb{Z}, \mathbb{Q}$ (for $q = 2$), \mathbb{L} (using \log_2), and $h\mathbb{H}$ for $h = \frac{1}{2}$



2.3.1 A Bound on the Time Scale Exponential

The magnitude of the time scale exponential on any time scale \mathbb{T} obeys the following inequality:

$$|e_\alpha(t)| \begin{cases} \leq e^{\alpha_r t}, & t \geq 0, \\ \geq e^{\alpha_r t}, & t \leq 0, \end{cases} \tag{2.6}$$

where $\alpha = \alpha_r + j\alpha_i$ and $\alpha_r = \text{Re } \alpha$ and $\alpha_i = \text{Im } \alpha$. For $t \geq 0$, this is graphically evident in Fig. 1 for the special case of $\alpha = 1$.

To show (2.6), we see from (2.4) that

$$\begin{aligned} |e_\alpha(t)| &= \left| \exp\left(\int_{\tau=0}^t \frac{\log(1 + \mu(\tau)\alpha)}{\mu(\tau)} \Delta\tau\right) \right| \\ &= \exp\left(\text{Re}\left\{\int_{\tau=0}^t \frac{\log(1 + \mu(\tau)\alpha)}{\mu(\tau)} \Delta\tau\right\}\right). \end{aligned} \tag{2.7}$$

Since

$$1 + \mu(\tau)\alpha = |1 + \mu(\tau)\alpha| \exp\left(j \arctan\left(\frac{\alpha_i}{1 + \mu(\tau)\alpha_r}\right)\right),$$

we have

$$\text{Re } \log((1 + \mu(\tau)\alpha)) = \frac{1}{2}(\log(1 + \mu(\tau)\alpha_r)^2 + (\mu(\tau)\alpha_i)^2)$$

and (2.7) becomes

$$\begin{aligned} |e_\alpha(t)| &= \exp\left(\frac{1}{2} \int_{\tau=0}^t \frac{\log((1 + \mu(\tau)\alpha_r)^2 + (\mu(\tau)\alpha_i)^2)}{\mu(\tau)} \Delta\tau\right) \\ &= \exp\left(\frac{1}{2} \int_{\tau=0}^t \frac{\log(1 + 2\mu(\tau)\alpha_r + (\mu(\tau)|\alpha|)^2)}{\mu(\tau)} \Delta\tau\right). \end{aligned}$$

When θ is real, $\log(1 + \theta) \leq \theta$, and we have, for $t \geq 0$,

$$\begin{aligned} |e_\alpha(t)| &\leq \exp\left(\frac{1}{2} \int_{\tau=0}^t \frac{2\mu(\tau)\alpha_r + (\mu(\tau)|\alpha|)^2}{\mu(\tau)} \Delta\tau\right) \\ &= \exp\left(\frac{1}{2} \int_{\tau=0}^t (2\alpha_r + \mu(\tau)|\alpha|^2) \Delta\tau\right). \end{aligned} \tag{2.8}$$

For $t \geq 0$,

$$|e_\alpha(t)| \leq \exp\left(\alpha_r \int_{\tau=0}^t \Delta\tau\right) = e^{\alpha_r t}.$$

Similar reasoning gives the results in (2.6) for $t \leq 0$.

2.3.2 The \ominus Operator

Define

$$q(t) \ominus p(t) := \frac{q(t) - p(t)}{1 + \mu(t)p(t)}. \tag{2.9}$$

Interpret $\ominus p(t)$ as (2.9) with $q(t) = 0$. This operator has the following useful properties that follow immediately from (2.4).

- The exponentiation reciprocation property is

$$\frac{1}{e_{p(t)}(t)} = e_{\ominus p(t)}(t). \tag{2.10}$$

- The exponential multiplication property is

$$e_{q(t)}(t)e_{\ominus p(t)}(t) = e_{q(t)\ominus p(t)}(t). \tag{2.11}$$

3 Unilateral Laplace Transforms on Time Scales

The *unilateral Laplace transform* on a time scale is defined as² [1]

$$F_u(z) = \int_{t=0}^{\infty} f(t)e_{\ominus z}^\sigma(t)\Delta t, \tag{3.1}$$

where we are using the notation $e_{\ominus z}^\sigma(t) := e_{\ominus z}(t^\sigma)$.

For $\mathbb{T} = \mathbb{R}^+$, the time scale Laplace transform takes on the familiar form of the continuous-time Laplace transform,

$$F_u(z) = \int_{t=0}^{\infty} f(t)e^{-zt} dt.$$

²The generalization of the Laplace transform in (3.1), popularized by Bohner and Peterson [1], contrasts with Hilger’s generalization of the Fourier transform on time scales [9] which we have considered elsewhere [5].

In discrete time, $\mathbb{T} = \mathbb{Z}^+$, we have $t = n$ and

$$F_u(z) = \sum_{n=0}^{\infty} f(n)(1+z)^{-(n+1)}.$$

The traditional unilateral z -transform [12] is

$$F_z(z) = \sum_{n=0}^{\infty} f(n)z^{-n}.$$

Thus,

$$F_u(z) = \frac{F_z(z+1)}{z+1} \quad (3.2)$$

so that the time scale Laplace transform on \mathbb{R}^+ is equivalent to a shift of the traditional unilateral z -transform scaled by $z+1$. We can equivalently write (3.2) as

$$F_z(z) = zF_u(z-1).$$

In this sense, the traditional continuous-time Laplace transform and the discrete-time z -transform are special cases of the time scale Laplace transform in (3.1).

3.1 The Hilger Circle

We first consider unilateral Laplace transforms of signals with *finite area* [12]. A signal on a time scale \mathbb{T} has finite area if

$$\int_{t \in \mathbb{T}} |f(t)| \Delta t < \infty.$$

Definition 3.1 The Hilger circle on the z plane is defined by the set of z satisfying

$$\left| z + \frac{1}{\mu} \right| = \frac{1}{\mu}. \quad (3.3)$$

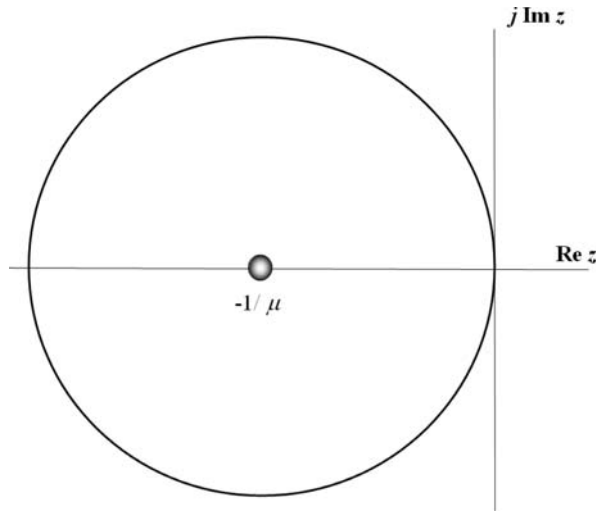
The Hilger circle is illustrated in Fig. 3. Its center is on the negative real, and the circle is tangent to the imaginary axis.

Theorem 3.1 (Unilateral Laplace transforms of finite area signals) *If a unilateral discrete signal on a time scale \mathbb{D} has finite area, then its unilateral Laplace transform converges, at least outside of the Hilger circle defined by graininess μ .*

Proof

$$\begin{aligned} |F_u(z)| &= \left| \int_0^{\infty} f(t) e_{\ominus z}^{\sigma}(t) \Delta t \right| \\ &\leq \int_0^{\infty} |f(t)| |e_{\ominus z}^{\sigma}(t)| \Delta t. \end{aligned} \quad (3.4)$$

Fig. 3 The Hilger circle



But for $t \geq 0$,

$$|e_{\ominus z}^\sigma(t)| = \prod_{k=0}^n |1 + \mu(t_k)z|^{-1}. \tag{3.5}$$

If each term in the product is less than one, then

$$|e_{\ominus z}^\sigma(t)| < 1. \tag{3.6}$$

Each term is less than one if

$$|1 + \mu(t_k)z| > 1,$$

or, equivalently,

$$\left| z + \frac{1}{\mu(t_k)} \right| > \frac{1}{\mu(t_k)}.$$

This is the set of all points external to the Hilger circle in Fig. 3. Then (3.4) becomes

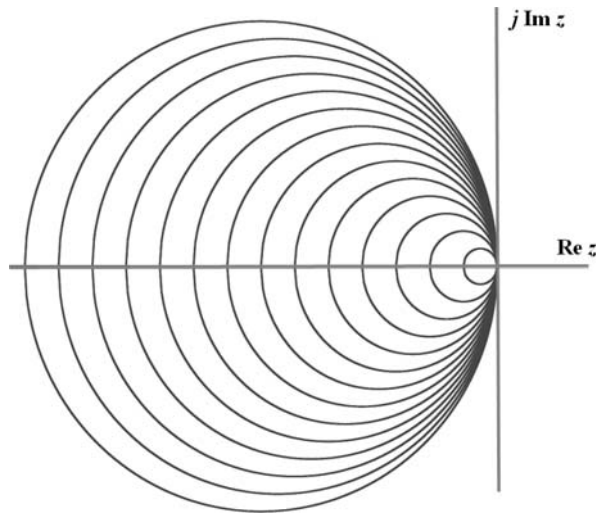
$$|F_u(z)| \leq \int_0^\infty |f(t)| \Delta t < \infty. \quad \square$$

3.1.1 The ROC on \mathbb{R} and \mathbb{Z}

The Hilger circle is instructive in illustrating how the time scale Laplace transform in (3.1) subsumes the continuous Laplace transform and the z -transform as special cases. As the graininess μ becomes smaller, we get closer and closer to \mathbb{R} . As $\mu \rightarrow 0$, the Hilger circle engulfs the entire left half-plane as we approach the continuous-time Laplace transform. We then obtain the familiar result that the Laplace transform of finite area signals converges in the right half-plane [12].

For the z -transform, the unit circle in the z plane plays a similar role to the left half-plane in the Laplace transform. For the causal discrete-time scale \mathbb{Z}^+ , $\mu = 1$ and

Fig. 4 A family of Hilger circles corresponding to varying graininess. As $\mu \rightarrow 0$, the Hilger circle's radius approaches infinity, thereby claiming the entire left half-plane



the Hilger circle in Fig. 3 is, indeed, a unit circle. The unit circle for the traditional z -transform, however, is centered and the Hilger circle is not. The reason is that the transformation in (3.2) shifts the unit circle to a unit radius Hilger circle. The familiar property of unilateral z -transforms of finite energy signals converging external to the unit circle is thus equivalent to such signals converging external to a unit radius Hilger circle.

3.1.2 The ROC of Finite Area Signals

The Hilger circle changes temporally from point to point. This is illustrated in Fig. 4. A *region of convergence* (ROC) for (3.6) is the intersection of the areas external to each of these circles, i.e., in the region external to the largest Hilger circle.

3.1.3 Graininess-independent ROC

Since $\mu \geq 0$, the ROC of the Laplace transform converges on at least the right half-plane independent of the time scale's graininess.

3.2 Unilateral Laplace Transforms of Exponentials

Before exploring the unilateral Laplace transform of a time scale exponential, we establish some preliminaries.

3.2.1 The Modified Hilger Circle

For a complex number, $\alpha = \alpha_r + j\alpha_i$, the modified Hilger circle in the z plane is the locus of points satisfying

$$\left| z + \frac{1}{\mu(t)} \right| = \left| \alpha + \frac{1}{\mu(t)} \right|. \quad (3.7)$$

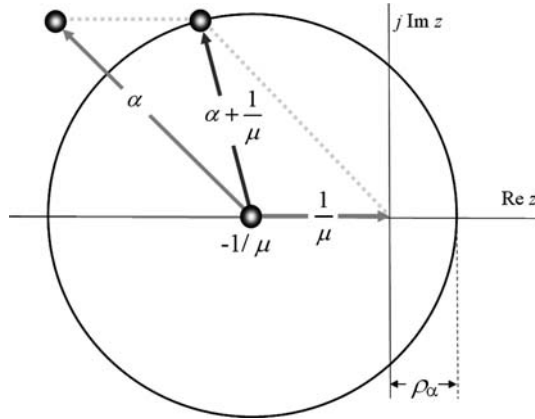


Fig. 5 An illustration of the modified Hilger circle defined in (3.7) for graininess μ and complex number α . The circle is centered at $-1/\mu$. Since $\mu > 0$, the circle's center is thus always on the nonpositive real z axis. We add the real numbers $1/\mu$ and α using the circle's midpoint as reference. The magnitude of the sum geometrically illustrated here using a parallelogram is the radius of the circle. The circle passes through α and its complex conjugate. The circle's center and α thus supply three points needed to uniquely define the circle

The modified Hilger circle is illustrated in Fig. 5. It has the following properties.

1. All modified Hilger circles pass through the points $z = \alpha$ and $z = \alpha^*$, where the asterisk denotes complex conjugation.
2. The Hilger circle in (3.3) is a special case for $\alpha = 0$.
3. When $\mu(t) = 0$, the modified Hilger circle surrounds all points to the left of the line $z = \alpha_r$.

For a fixed α and varying graininess, a family of modified Hilger circles is illustrated in Fig. 6 for $\alpha_r > 0$. The smallest circle has its center at the origin ($\mu = \infty$). The largest circle, corresponding to $\mu = 0$, has an infinite radius.

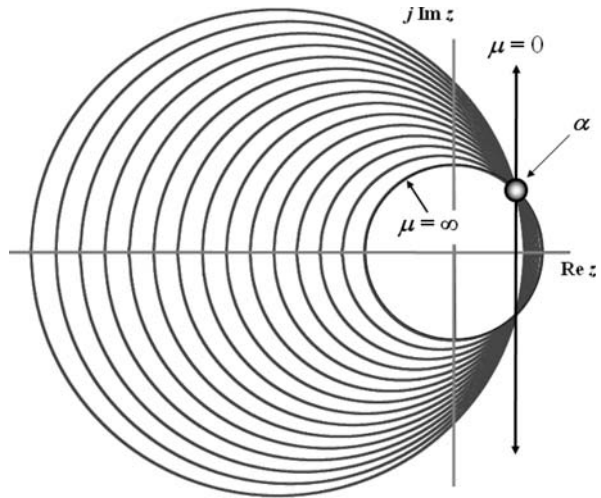
As illustrated in Fig. 8, the family of modified Hilger circles has a different character when $\alpha_r < 0$. The modified Hilger circle attains its smallest radius, $|\alpha_i|$, when $\alpha_r = -1/\mu$. On each side of this smallest circle, the diameters grow. To the left the diameters grow without bound reaching, in the limit, a circle of infinite radius corresponding to all points to the left of the line defined by $z = \alpha_r$. This is shown in Fig. 6. To the right of the smallest circle, the circles increase in diameter until the point where the circle's center is at the origin ($\mu = 0$).

3.2.2 The Nonregressive Case

When $\alpha_r < 0$ and $\alpha_i = 0$, the modified Hilger circles in Fig. 8 can pinch to zero diameter at the point corresponding to

$$\alpha_r = -\frac{1}{\mu(t)}. \tag{3.8}$$

Fig. 6 A family of modified Hilger circles for a fixed α and various values of graininess. This example assumes $\alpha_r > 0$. An $\alpha_r < 0$ case is illustrated in Fig. 8



The exponential function is then said to be *nonregressive* at this point [1]. From (2.5), for $t \geq 0$,

$$e_\alpha(t_n) = \prod_{k=0}^{n-1} (1 + \mu(t_k)\alpha). \tag{3.9}$$

At a point of nonregression, say $t = t_k^*$, we have $1 + \mu(t_k^*)\alpha = 0$ and (3.8) is true. Then, for $t \geq t_k^*$, it follows immediately from (3.9) that

$$e_\alpha(t_n) = 0 \quad \text{for } t_n \geq t_k^*.$$

The exponential therefore hits zero and stays there. Nonregressivity always occurs at

$$z = -\frac{1}{\mu(t_k)}$$

for $0 \leq k < \infty$. These are isolated points on the negative real axis on the z plane.

At nonregressive points, the Laplace transform kernel contains a pole.³

$$|e_{\ominus\alpha}^\sigma(t)| = \left| \frac{1}{e_\alpha^\sigma(t)} \right| = \infty.$$

Nonregressivity occurs in dynamic electrical and mechanical systems [10]. For continuous time, the graininess is zero and all functions on \mathbb{R} are regressive.

³As we show later, however, this pole lies outside of the region of convergence of the transform.

3.2.3 Graininess Bounds

We denote the region in the z plane external to the modified Hilger circle by $\mathcal{H}(\alpha, \mu)$. Define the intersection of two such regions by

$$\mathcal{R}(\alpha, \mu_1, \mu_2) = \mathcal{H}(\alpha, \mu_1) \cap \mathcal{H}(\alpha, \mu_2). \tag{3.10}$$

Some properties of \mathcal{R} follow.

1. *Relation to modified Hilger circle:*

$$\mathcal{R}(\alpha, \mu, \mu) = \mathcal{H}(\alpha, \mu). \tag{3.11}$$

2. *Limit:* The region

$$\mathcal{D}(\alpha) := \mathcal{R}(\alpha, 0, \infty) \tag{3.12}$$

is a *dimpled half-plane* consisting of all the points external to a circle with radius $|\alpha|$ centered at the origin intersected with the points on the half-plane to the right of the line $z = \alpha_r$. Examples are illustrated in Fig. 7 for various values of α .

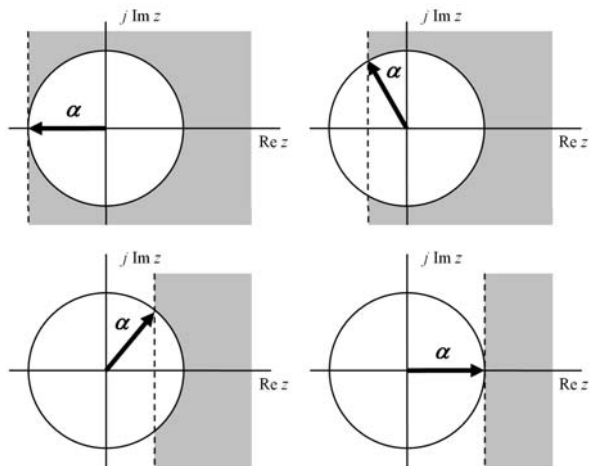
3. *Nonnegative argument:* When α is real and positive, note that $\mathcal{D}(\alpha)$ is a half-plane of all points to the left of the line $z = \alpha$. This is illustrated in the lower right figure in Fig. 7.

Lemma 3.1 Let $\mu(t)$ be bounded by⁴

$$\dot{\mu} \leq \mu(t) \leq \dot{\mu}.$$

For a fixed α , the union of the set of values of z external to all of the modified Hilger circles in this interval is equal to the intersection of values of z external to two circles

Fig. 7 Examples of dimpled half-planes, $\mathcal{D}(\alpha)$, shown shaded



⁴The slash over the μ in $\dot{\mu}$ goes up denoting an upper bound. Likewise, $\dot{\mu}$ denotes the lower bound.

Fig. 8 The family of modified Hilger circles for $\alpha = \alpha_r + j\alpha_i$ when $\alpha_r < 0$

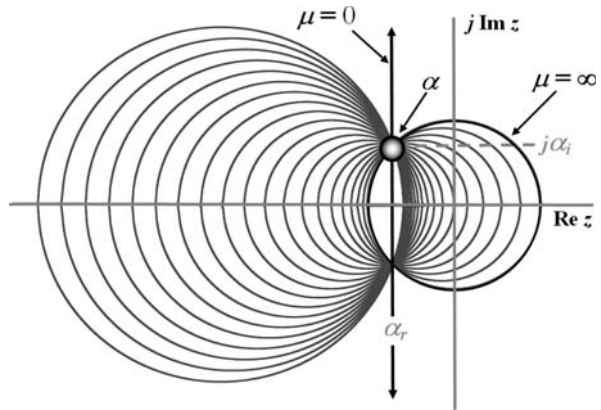
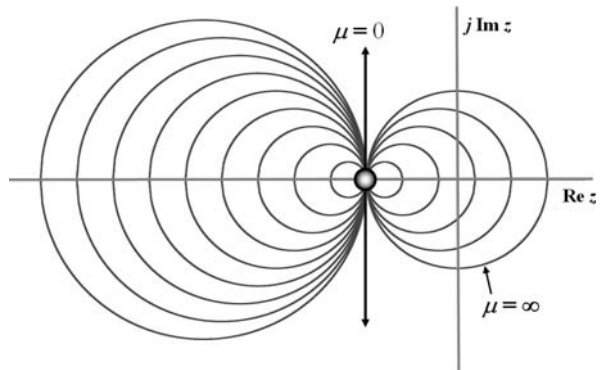


Fig. 9 Nonregressivity can occur when the α is negative and real. At this point, the modified Hilger circle has zero diameter and the time scale exponential hits zero and stays there



parameterized by $\dot{\mu}$ and $\acute{\mu}$,

$$\bigcap_{\dot{\mu} \leq \mu(t) \leq \acute{\mu}} \mathcal{H}(\alpha, \mu(t)) = \mathcal{R}(\alpha, \dot{\mu}, \acute{\mu}).$$

In Fig. 10, two circles on the z plane, centered at c and

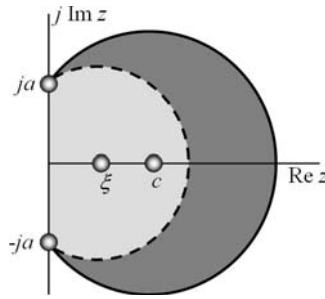
$$\xi < c, \tag{3.13}$$

are shown. Both go through the point $z = ja$ and then, by necessity, $z = -ja$. To prove Lemma 3.1, we need only show that, for $z_r \geq 0$, the smaller circle is totally subsumed in the larger. Then, with reference to Figs. 6, 8, and 9, all modified Hilger circles to the left of α_r are subsumed in the rightmost circle for $z_r \geq \alpha_r$. Likewise, imposing a mirror image of Fig. 10, all modified Hilger circles to the right of α_r are subsumed in the leftmost circle for $z_r \leq \alpha_r$. In Fig. 10 we have set $\alpha_r = 0$ with no loss of generality.

Proof We first note that the larger circle in Fig. 10 contains the set of all points for which

$$|z - c| \leq |ja - c|.$$

Fig. 10 Figure used in the proof of Lemma 3.1



Squaring and expanding straightforwardly gives

$$|z|^2 \leq a^2 + 2cz_r.$$

Subtracting $(2\xi z_r - \xi^2)$ from both sides gives

$$|z - \xi|^2 \leq |ja - \xi|^2 - 2(c - \xi)z_r.$$

Using (3.13), we conclude that

$$|z - \xi|^2 \leq |ja - \xi|^2 \quad \text{for } z^r \geq 0.$$

This is the equation for all points subsumed in the smaller circle in Fig. 10, and the proof is complete. \square

Lemma 3.1 is geometrically self-evident after inspection of Figs. 6, 8, and 9. In all cases, the values of z external to all of the circles is the same as the points external to the leftmost and rightmost circles.

For a given time scale, we make the following definitions.

- (a) The *entire graininess lower bound*, $\hat{\mu}_+^0$, for causal time scales is⁵

$$\hat{\mu}_+^0 = \inf_{t \in \mathbb{T}^+} \mu(t).$$

Similarly, the *entire graininess upper bound*, $\hat{\mu}_+^0$, is

$$\hat{\mu}_+^0 = \sup_{t \in \mathbb{T}^+} \mu(t).$$

- (b) Time scales with an *attained graininess lower bound* have a lower bound on graininess for times greater than some finite T . The attained graininess lower bound is

$$\hat{\mu}_+^T = \inf_{t \in \mathbb{T}^+, t \geq T} \mu(t).$$

⁵The subscript “+” denotes positive time. In a treatment of bilateral Laplace transforms, the subscript “-” will denote negative time.

The attained graininess upper bound is

$$\hat{\mu}_+^T = \sup_{t \in \mathbb{T}^+, t \geq T} \mu(t).$$

Some special cases follow.

- (i) The asymptotic graininess lower bound for causal time scales is

$$\begin{aligned} |F_u(z)| &= \lim_{T \rightarrow \infty} \hat{\mu}_+^T \\ &= \lim_{T \rightarrow \infty} \inf_{t \in \mathbb{T}^+, t \geq T} \mu(t). \end{aligned}$$

Thus,

$$\hat{\mu}_+^0 \leq \hat{\mu}_+^T \leq \hat{\mu}_+^\infty. \tag{3.14}$$

The corresponding asymptotic graininess upper bound is

$$\begin{aligned} \hat{\mu}_+^\infty &= \lim_{T \rightarrow \infty} \hat{\mu}_+^T \\ &= \lim_{T \rightarrow \infty} \sup_{t \in \mathbb{T}^+, t \geq T} \mu(t), \end{aligned}$$

so that

$$\hat{\mu}_+^0 \geq \hat{\mu}_+^T \geq \hat{\mu}_+^\infty. \tag{3.15}$$

- (ii) If $\hat{\mu}_+^\infty = \hat{\mu}_+^0$, then the time scale is said to have a constant asymptotic graininess,

$$\bar{\mu}_+^\infty = \hat{\mu}_+^\infty = \hat{\mu}_+^0.$$

Some graininess measures for some selected time scales are listed in Table 1. The following lemmas establish sufficient conditions for

$$\lim_{t \rightarrow \infty} e_{\alpha \ominus z}(t) = 0. \tag{3.16}$$

This region is useful in finding the ROC of the unilateral Laplace transform of $e_\alpha(t)$.

Lemma 3.2 (Time scale-dependent ROCs: the entire case) *A sufficient condition for (3.16) is that*

$$z \in \mathcal{R}(\alpha, \hat{\mu}_+^0, \hat{\mu}_+^0). \tag{3.17}$$

Table 1 Graininess measures for some example time scales. The entry “ND” denotes “not defined”

Time Scale	$\hat{\mu}_+^0$	$\hat{\mu}_+^0$	$\hat{\mu}_+^\infty$	$\hat{\mu}_+^\infty$	$\bar{\mu}_+^\infty$
\mathbb{Z}	1	1	1	1	1
\mathbb{L}	0	$\log(2)$	0	0	0
\mathbb{H}	0	1	0	0	0
\mathbb{P}	0	$1 - \lambda$	0	$1 - \lambda$	ND
\mathbb{Q}	1	∞	∞	∞	∞
\mathbb{R}	0	0	0	0	0

Proof From (2.5),

$$e_{\alpha \ominus z}(\infty) = \prod_{k=0}^{\infty} \frac{1 + \alpha \mu(t_k)}{1 + z \mu(t_k)}. \tag{3.18}$$

When (3.17) is true, z lies external to every modified Hilger circle for every $\mu(t)$. Each of the terms in (3.18) is strictly less than one and the product therefore tends to zero. \square

Lemma 3.3 (Time scale-dependent ROCs: the local case) *A sufficient condition for (3.16) is that*

$$z \in \mathcal{R}(\alpha, \dot{\mu}_+^T, \acute{\mu}_+^T). \tag{3.19}$$

Proof We can write (3.18) as

$$e_{\alpha \ominus z}(\infty) = \prod_{t_k < T} \frac{1 + \alpha \mu(t_k)}{1 + z \mu(t_k)} \times \prod_{t_k \geq T}^{\infty} \frac{1 + \alpha \mu(t_k)}{1 + z \mu(t_k)}; \quad t_k \geq 0. \tag{3.20}$$

If the second term is zero, then

$$\lim_{t \rightarrow \infty} e_{\alpha \ominus z}(t) = 0.$$

Using the same reasoning as in Lemma 3.2, this is achieved when (3.19) is true. \square

Lemma 3.4 (Time scale-dependent ROCs: the asymptotic case) *A sufficient condition for (3.16) is that*

$$z \in \mathcal{R}(\alpha, \dot{\mu}_+^{\infty}, \acute{\mu}_+^{\infty}). \tag{3.21}$$

Proof This follows as the asymptotic case of Lemma 3.3. \square

Lemma 3.5 (Time scale-independent ROCs: the global case) *For all causal time scales, (3.16) is true for*

$$z \in \mathcal{D}(\alpha). \tag{3.22}$$

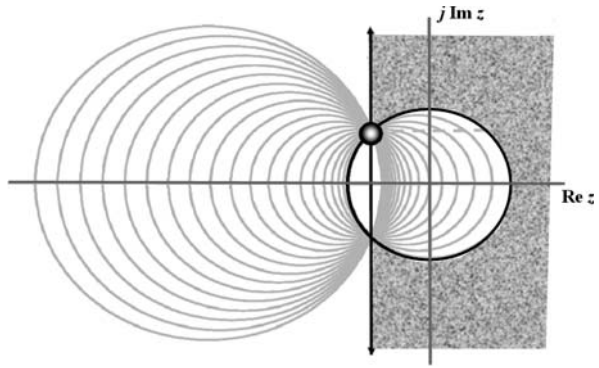
This dimpled half-plane ROC, illustrated in Fig. 11 and, for various α in Fig. 7, is applicable to all time scales.

Proof This follows from (2.2) and Lemma 3.1. \square

Lemma 3.6 *From Lemmas 3.2, 3.3, 3.4, and 3.5,*

$$\begin{aligned} \mathcal{D}(\alpha) &\subseteq \mathcal{R}(\alpha, \dot{\mu}_+^0, \acute{\mu}_+^0) \\ &\subseteq \mathcal{R}(\alpha, \dot{\mu}_+^T, \acute{\mu}_+^T) \\ &\subseteq \mathcal{R}(\alpha, \dot{\mu}_+^{\infty}, \acute{\mu}_+^{\infty}). \end{aligned}$$

Fig. 11 Illustration of a dimpled half-plane, $\mathcal{D}(\alpha)$, where the small dot denotes the location of the complex number α . The unilateral Laplace transform of $e_\alpha(t)$ converges at least in the shaded area shown here. The value of α is the same as used in Fig. 8



The largest ROCs thus occur using asymptotic graininess upper and lower bounds.

Proof The proof follows immediately from the graininess inequalities in (2.2), (3.14), and (3.15), and Lemma 3.1. □

Lemma 3.7 *When a time scale has a constant asymptotic graininess $\bar{\mu}_+^\infty$, then (3.16) is true for*

$$z \in \mathcal{H}(\alpha, \bar{\mu}_+^\infty),$$

in other words, to values external to a modified Hilger circle.

Proof The proof follows from (3.11) and Lemma 3.5. □

We are now ready to establish a major theorem.

Theorem 3.2 *For a causal time scale, \mathbb{T}^+ , let $f(t) = e_\alpha(t)$. Then the corresponding unilateral Laplace transform is*

$$F_u(z) = \frac{1}{z - \alpha}, \tag{3.23}$$

where convergence is in one of the regions defined in Lemmas 3.2, 3.3, 3.4, 3.5, or 3.7.

Proof

$$\begin{aligned} F_u(z) &= \int_0^\infty e_\alpha(t) e_{\ominus t}^\sigma(t) \Delta t \\ &= \int_0^\infty (1 + \mu(t)z)^{-1} e_\alpha(t) e_{\ominus t}(t) \Delta t \\ &= \int_0^\infty (1 + \mu(t)z)^{-1} e_{\alpha \ominus t}(t) \Delta t \end{aligned}$$

$$\begin{aligned}
 &= \frac{1}{\alpha - z} \int_0^\infty \frac{\alpha - z}{1 + \mu(t)z} e_{\alpha \ominus t}(t) \Delta t \\
 &= \frac{1}{\alpha - z} \int_0^\infty (\alpha \ominus z) e_{\alpha \ominus t}(t) \Delta t \\
 &= \frac{1}{\alpha - z} e_{\alpha \ominus t}(t) \Big|_0^\infty. \quad \square
 \end{aligned}$$

For the ROCs in Lemmas 3.2, 3.3, 3.4, 3.5, or 3.7, we have $e_{\alpha \ominus t}(\infty) = 0$. Since $e_{\alpha \ominus t}(0) = 1$, (3.23) results.

4 Other Transcendental Functions on Time Scales

Other transcendental functions on a time scale are listed in Table 2. Some unilateral Laplace transforms based on these functions are listed in Table 3. Remarkably, the time scale Laplace transform function is independent of time scale [1, 5]. The time scale, however, determines the ROC on the z plane.

Derivations of the entries in Table 3 on the z plane follow. In this section, we set⁶ $\alpha_i = \omega$ and $\alpha_r = a$. We also define, for real a

$$w := \omega \ominus a - \ominus a.$$

Table 2 Some transcendental functions on a time scale. For \mathbb{R} , $e_z(t) = e^{zt}$. Therefore, on \mathbb{R} , $\cos_\omega(t) = \cos(\omega t)$, $\sin_\omega(t) = \sin(\omega t)$, $\cosh_a(t) = \cosh(at)$, and $\sinh_a(t) = \sinh(at)$

(a)	$u(t) = 1$ for $t \geq 0$ and 0 otherwise
(b)	$\cos_\omega(t) = \frac{1}{2}(e_{j\omega}(t) + e_{-j\omega}(t))$
(c)	$\sin_\omega(t) = \frac{1}{j2}(e_{j\omega}(t) - e_{-j\omega}(t))$
(d)	$\cosh_a(t) = \frac{1}{2}(e_a(t) + e_{-a}(t))$
(e)	$\sinh_a(t) = \frac{1}{2}(e_a(t) - e_{-a}(t))$

Table 3 Some transcendental functions on an arbitrary time scale and their unilateral Laplace transforms. $w := \omega \ominus a - \ominus a = \frac{\omega}{1 + \mu(t)a}$. On \mathbb{R} , we have $w = \omega$

(1)	$u(t) \longleftrightarrow \frac{1}{z}$
(2)	$\cos_\omega(t) \longleftrightarrow \frac{z}{z^2 + \omega^2}$
(3)	$\sin_\omega(t) \longleftrightarrow \frac{\omega}{z^2 + \omega^2}$
(4)	$\cosh_a(t) \longleftrightarrow \frac{z}{z^2 - a^2}$
(5)	$\sinh_a(t) \longleftrightarrow \frac{a}{z^2 - a^2}$
(6)	$e_a(t) \cos_w(t) \longleftrightarrow \frac{z - a}{(z - a)^2 + \omega^2}$
(7)	$e_a(t) \sin_w(t) \longleftrightarrow \frac{\beta}{(z - a)^2 + \omega^2}$
(8)	$e_a(t) \cosh_w(t) \longleftrightarrow \frac{z - a}{(z - a)^2 - \omega^2}$
(9)	$e_a(t) \sinh_w(t) \longleftrightarrow \frac{w}{(z - a)^2 - \omega^2}$

⁶The variable $\sigma = \alpha_r$ is more commonly used in continuous time Laplace transforms, but its use here would invite confusion with the forward jump operator in (2.1).

For each of the functions in Table 3, three ROCs will be derived.

- *Bounded ROC*: This ROC is applicable when the time scale has asymptotic graininess upper and lower bounds of $\hat{\mu}_+^\infty$ and $\check{\mu}_+^\infty$. The ROCs are parameterized by these bounds. Smaller ROCs can be obtained by using the same ROCs parameterized by either $\hat{\mu}_+^T$ and $\check{\mu}_+^T$, or $\hat{\mu}_+^0$ and $\check{\mu}_+^0$.
- *Asymptotic ROC*: These ROCs are applicable to time scales with a fixed asymptotic graininess $\bar{\mu}_+^\infty$.
- *Global ROC*: Since $\hat{\mu}_+^\infty \geq 0$ and $\check{\mu}_+^\infty \leq \infty$, the global ROC is obtained from the bounded ROC by using these extreme values. The global ROC is therefore independent of the time scale used.

We now derive each entry in Table 3 and establish their various ROCs.

(1) $u(t)$

The transform of the unit step, $u(t)$, follows immediately from (3.23) after recognizing that, for $t \geq 0$,

$$e_\alpha(t)|_{\alpha=0} = u(t).$$

- *Bounded ROC*: From the bounded ROC for $e_\alpha(t)$, we immediately recognize that the bounded ROC for the unit step is $\mathcal{R}(0, \hat{\mu}_+^\infty, \check{\mu}_+^\infty)$. But the modified Hilger circle centered at $-1/\check{\mu}_+^\infty$ and going through the origin subsumes the circle centered at $-1/\hat{\mu}_+^\infty$, so the bounded ROC is $\mathcal{H}(0, \hat{\mu}_+^\infty)$.
- *Asymptotic ROC*: $\mathcal{H}(0, \bar{\mu}_+^\infty)$.
- *Global ROC*: The right half-plane $\mathcal{D}(0)$.

(2) $\cos_\omega(t)$

Applying (3.23) to definition (b) in Table 2 gives

$$\cos_\omega(t) \leftrightarrow \frac{1}{2} \left(\frac{1}{z - j\omega} + \frac{1}{z + j\omega} \right)$$

from which the transform of $\cos_\omega(t)$ in Table 3 follows.

- *Bounded ROC*: As illustrated in Fig. 12, the bounded ROC is $\mathcal{R}(j\omega, \hat{\mu}_+^\infty, \check{\mu}_+^\infty)$.
- *Asymptotic ROC*: The modified Hilger circle, $\mathcal{H}(j\omega, \bar{\mu}_+^\infty)$.
- *Global ROC*: The dimpled half-plane, $\mathcal{D}(j\omega)$.

(3) $\sin_\omega(t)$

The Laplace transform of $\sin_\omega(t)$ follows similarly. We have

$$\sin_\omega(t) \leftrightarrow \frac{1}{j2} \left(\frac{1}{z - j\omega} - \frac{1}{z + j\omega} \right).$$

The three ROCs are the same as for $\cos_\omega(t)$.

(4) $\cosh_a(t)$

Applying (3.23) in Table 2 gives

$$\cosh_a(t) \leftrightarrow \frac{1}{2} \left(\frac{1}{z - a} + \frac{1}{z + a} \right)$$

Fig. 12 The bounded ROC for $\cos_\omega(t)$ and $\sin_\omega(t)$ is shown shaded

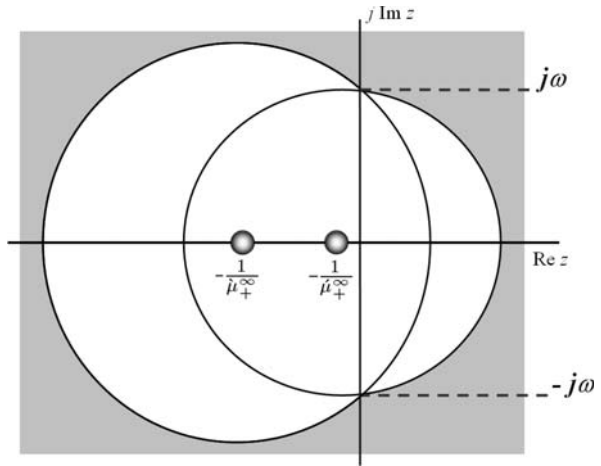
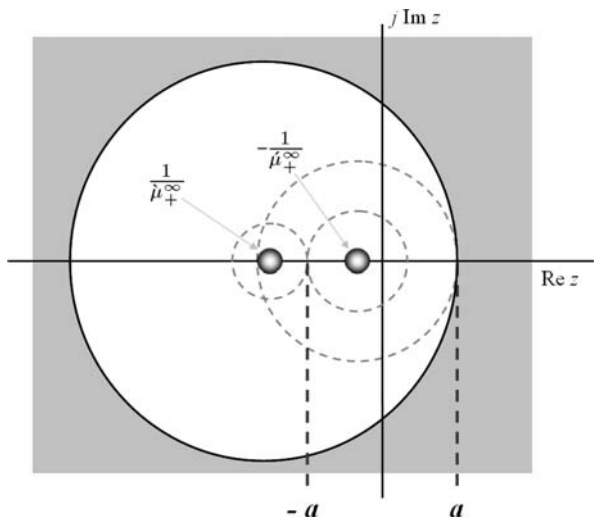


Fig. 13 The bounded ROC for $\cosh_a(t)$ and $\sinh_a(t)$ is $\mathcal{H}(|a|, \mu_+^\infty)$. This figure assumes $a > 0$



from which the transform of $\cosh_\omega(t)$ in Table 3 follows.

- **Bounded ROC:** For real a , the bounded ROC is $\mathcal{H}(|a|, \mu_+^\infty)$. This is illustrated in Fig. 13.
- **Asymptotic ROC:** This follows immediately as $\mathcal{H}(|a|, \bar{\mu}_+^\infty)$
- **Global ROC:** Then the global ROC follows as the half-plane $\mathcal{D}(|a|)$.

(5) $\sinh_\omega(t)$
 Since

$$\sinh_a(t) \leftrightarrow \frac{1}{2} \left(\frac{1}{z-a} - \frac{1}{z+a} \right)$$

the Laplace transform in Table 3 follows immediately. The ROCs are the same as those for $\cosh_\omega(t)$.

(6) $e_a(t) \cos_w(t)$

This entry follows immediately from (3.23) after recognizing that

$$e_a(t) \cos_w(t) = \frac{1}{2} (e_\alpha(t) + e_{\alpha^*}(t)).$$

- *Bounded ROC*: The bounded ROC is $\mathcal{R}(\alpha, \dot{\mu}_+^\infty, \dot{\mu}_+^\infty)$.
- *Asymptotic ROC*: $\mathcal{H}(\alpha, \bar{\mu}_+^\infty)$.
- *Global ROC*: $\mathcal{D}(\alpha)$.

(7) $e_a(t) \sin_w(t)$

Since

$$e_a(t) \sin_w(t) = \frac{1}{j2} (e_\alpha(t) - e_{\alpha^*}(t)),$$

the ROCs here are the same as for $e_a(t) \cos_w(t)$.

(8) $e_a(t) \cosh_w(t)$

Since

$$e_a(t) \cosh_w(t) = \frac{1}{2} (e_{a+\omega}(t) + e_{a-\omega}(t)), \tag{4.1}$$

the entry in Fig. 13 follows. We find it useful to define

$$b_+ = \max(a - \omega, a + \omega)$$

and

$$b_- = \min(a - \omega, a + \omega).$$

- *Bounded ROC*: The bounded ROC is the intersection of two \mathcal{R} 's in (4.1).

$$\mathcal{C}_{\mathcal{R}} := \mathcal{R}(b_+, \dot{\mu}_+^\infty, \dot{\mu}_+^\infty) \cap \mathcal{R}(b_-, \dot{\mu}_+^\infty, \dot{\mu}_+^\infty). \tag{4.2}$$

This bounded ROC for $e_a(t) \cosh_w(t)$ can be the exterior of a single modified Hilger circle or the exterior of two Hilger circles. This is illustrated in Fig. 14.

- *Asymptotic ROC*: Using (3.11), the ROC for time scales with a constant asymptotic graininess is, from (4.2),

$$\begin{aligned} \mathcal{C}_{\mathcal{H}} &:= \mathcal{C}_{\mathcal{R}} |_{\dot{\mu}_+^\infty = \bar{\mu}_+^\infty = \bar{\mu}_+^\infty} \\ &= \mathcal{H}(b_+, \bar{\mu}_+^\infty) \cap \mathcal{H}(b_-, \bar{\mu}_+^\infty). \end{aligned}$$

- *Global ROC*: Using (3.12) applied to (4.2) reveals the global ROC for $e_a(t) \cosh_w(t)$ as

$$\begin{aligned} \mathcal{C}_{\mathcal{D}} &:= \mathcal{C}_{\mathcal{R}} |_{\dot{\mu}_+^\infty = 0, \dot{\mu}_+^\infty = \infty} \\ &= \mathcal{D}(b_+) \cap \mathcal{D}(b_-). \end{aligned} \tag{4.3}$$

Some examples of $\mathcal{C}_{\mathcal{D}}$ are illustrated in Fig. 15.

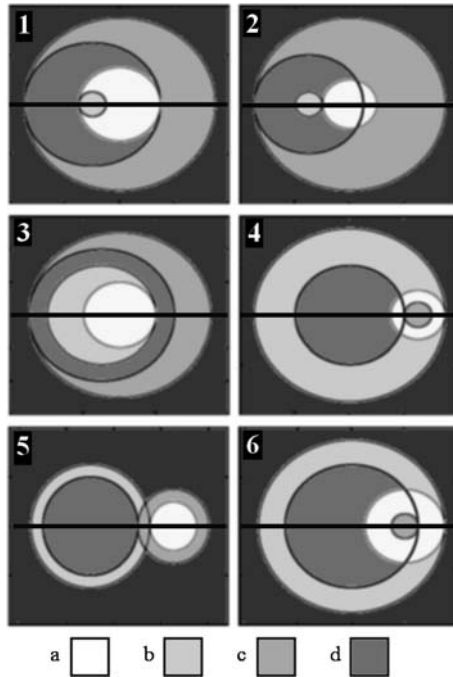


Fig. 14 Different ROCs for $e_a(t) \cosh_w(t)$ and $e_a(t) \sinh_w(t)$ are shown as *black*. There are four parameters. (i) the centers of the circles, $\hat{c} := -1/\hat{\mu}_+^\infty$ and (ii) $\acute{c} := -1/\acute{\mu}_+^\infty$; and (iii) the parameters of the function $b_+ := a + \omega$ and (iv) $b_- := a - \omega$. Since $\hat{\mu}_+^\infty \leq \acute{\mu}_+^\infty$, we also know that $\hat{c} \leq \acute{c}$. There are four circles involved in each bounded ROC. Each circle is concentric with a second circle and tangent with a third either at b_- or b_+ . They are shaded using the **(a, b, c, d)** key shown at the bottom of the figure as modified Hilger circles **(a)** $\mathcal{H}(b_+, \hat{\mu}_+^\infty)$, **(b)** $\mathcal{H}(b_+, \acute{\mu}_+^\infty)$, **(c)** $\mathcal{H}(b_-, \hat{\mu}_+^\infty)$, and **(d)** $\mathcal{H}(b_-, \acute{\mu}_+^\infty)$. The two ROCs in (4.2) follow as $\mathcal{R}(b_+, \hat{\mu}_+^\infty, \acute{\mu}_+^\infty) =$ points external to both circles **(a)** and **(b)**, while $\mathcal{R}(b_-, \hat{\mu}_+^\infty, \acute{\mu}_+^\infty)$ corresponds to points external to circles **(c)** and **(d)**. The intersection of these regions, denoted by \mathcal{C} in (4.2), is shown in the above figures as *shaded black*. With the four parameters and inequality constraints, there are six possible orderings. The figures above are instantiations of each. (1) For $b_- < b_+ < c_- < c_+$ as shown here, $\mathcal{C}_{\mathcal{R}} = \mathcal{H}(b_-, \hat{\mu}_+^\infty)$ (i.e., points exterior to circle **(c)**). (2) We obtain the same results for $b_- < c_- < b_+ < c_+$ as shown here, (3) and for $b_- < c_- < c_+ < b_+$. (4) For $c_- < b_- < c_+ < b_+$ as shown here, $\mathcal{C}_{\mathcal{R}} = \mathcal{H}(b_+, \hat{\mu}_+^\infty)$ (i.e., points exterior to circle **(b)**). (5) $c_- < c_+ < b_- < b_+$ for the example shown here has $\mathcal{C}_{\mathcal{R}} = \mathcal{H}(b_-, \hat{\mu}_+^\infty) \cap \mathcal{H}(b_+, \acute{\mu}_+^\infty)$ (i.e., points exterior to both circles **(b)** and **(c)**). (6) Lastly, for $c_- < c_+ < b_- < b_+$ as shown here, the result is the same as (4)

(9) $e_a(t) \sinh_w(t)$
 Similarly,

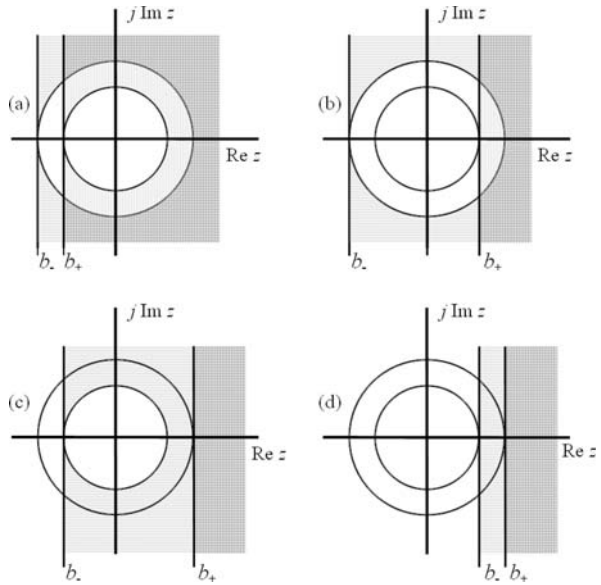
$$e_a(t) \sinh_w(t) = \frac{1}{j2} (e_{a+\omega}(t) - e_{a-\omega}(t)),$$

in Fig. 13 follows. The ROCs are the same as for $e_a(t) \cosh_w(t)$.

5 Extrapolation of the ROC

For the Laplace transform on \mathbb{R} , convergence of $F_u(z)$ at some value $z = \alpha$ ensures convergence on the half-plane $\text{Re } z \geq \alpha$. Likewise, for the conventional z -transform,

Fig. 15 Some examples of global ROCs, \mathcal{C}_D , for $e_a(t) \cosh_w(t)$ and $e_a(t) \sinh_w(t)$ given in (4.3). In each case, the ROC $\mathcal{D}(b_-)$ is shown shaded with horizontal lines and $\mathcal{D}(b_+)$ with vertical lines. The intersection of the two regions, \mathcal{C}_D , is shaded with crisscrossed horizontal and vertical lines. (a) When $b_- < b_+ < 0$, the global ROC is the intersection of points external to the larger circle and points to the right of b_+ . (b) For $b_- < 0$ and $-b_- > b_+ > 0$, the global ROC is likewise described. For (c) $b_- < 0$ and $-b_- < b_+ > 0$, and (d) $0 < b_- < b_+$, the global ROC is the set of points to the right of the line $z = b_+$



convergence at a point $z = \alpha$ ensures convergence for all $|z| \geq |\alpha|$. In this section, we present a generalization of this extrapolation for the general Laplace transform on a time scale.

Definition 5.1 A causal signal, $f(t)$, is said to display *strong convergence* at α on a time scale \mathbb{T} at time $t = T^\sigma$ if

$$\int_{T^\sigma}^\infty |f(t)e_{\ominus\alpha}^\sigma(t)| \Delta t < \infty.$$

Lemma 5.1 If $e_{\ominus\alpha}^\sigma(t)$ is regressive, then if $f(t)$ is bounded and displays strong convergence at T^σ , then $F_u(z)$ converges at $z = \alpha$.

Proof

$$\begin{aligned} |F_u(\alpha)| &= \left| \int_0^\infty f(t)e_{\ominus\alpha}^\sigma(t) \Delta t \right| \\ &\leq \left| \left[\int_0^{T^\sigma} + \int_{T^\sigma}^\infty \right] f(t)e_{\ominus\alpha}^\sigma(t) \Delta t \right| \\ &\leq \left| \int_0^{T^\sigma} f(t)e_{\ominus\alpha}^\sigma(t) \Delta t \right| \\ &\quad + \left| \int_{T^\sigma}^\infty f(t)e_{\ominus\alpha}^\sigma(t) \Delta t \right| \end{aligned}$$

$$\begin{aligned} &\leq \left| \int_0^T f(t)e_{\Theta z}^\sigma(t)\Delta t \right| \\ &\quad + \int_{T^\sigma}^\infty |f(t)e_{\Theta z}^\sigma(t)|\Delta t. \end{aligned} \tag{5.1}$$

If $e_z(t)$ is regressive, then $e_{\Theta z}^\sigma(t)$ is bounded. If $f(t)$ is also bounded, then the first integral in (5.1) is finite. The second integral is bounded by assumption. Thus, $|F_u(\alpha)| < \infty$. \square

Theorem 5.1 *If $|F_u(\alpha)| < \infty$, then $F_u(z)$ converges in the α parameterized ROCs defined in Lemmas 3.2, 3.3, 3.4, 3.5, and 3.7 dependent on the graininess properties of the time scale.*

Proof We have

$$\begin{aligned} |F_u(z)| &= \left| \int_0^\infty f(t)e_{\Theta z}^\sigma(t) \right| \\ &= \left| \left[\int_0^T + \int_{T^\sigma}^\infty \right] f(t)e_{\Theta z}^\sigma(t)\Delta t \right| \\ &\leq \left| \int_0^T f(t)e_{\Theta z}^\sigma(t)\Delta t \right| \\ &\quad + \left| \int_{T^\sigma}^\infty f(t)e_{\Theta z}^\sigma(t)\Delta t \right| \\ &\leq \left| \int_0^T f(t)e_{\Theta z}^\sigma(t)\Delta t \right| \\ &\quad + \left| \int_{T^\sigma}^\infty f(t)e_{\Theta\alpha}^\sigma e_{\alpha\Theta z}^\sigma(t)\Delta t \right| \\ &\leq \left| \int_0^T f(t)e_{\Theta z}^\sigma(t)\Delta t \right| \\ &\quad + \int_{T^\sigma}^\infty |f(t)e_{\Theta\alpha}^\sigma e_{\alpha\Theta z}^\sigma(t)|\Delta t, \end{aligned} \tag{5.2}$$

where we have used (2.10) and (2.11). If

$$|e_{\alpha\Theta z}^\sigma(t)| \leq 1, \tag{5.3}$$

then

$$\begin{aligned} |F_u(z)| &\leq \left| \int_0^T f(t)e_{\Theta z}^\sigma(t)\Delta t \right| \\ &\quad + \int_{T^\sigma}^\infty |f(t)e_{\Theta\alpha}^\sigma|\Delta t. \end{aligned} \tag{5.4}$$

This leads to the same ROCs as Lemmas 3.2, 3.3, 3.4, 3.5, and 3.7 dependent on the graininess properties of the time scale. \square

6 Conclusions

The following ROC properties for unilateral Laplace transformation of signals on time scales have been established.

1. Unilateral Laplace transforms of signals with finite area converge external to a Hilger circle. See Theorem 3.1.
2. Independent of graininess, the Laplace transform of a finite area signal always converges in the right half z plane. See Sect. 3.1.3.
3. The ROCs of Laplace transforms on time scales become the familiar half-plane and unit circle for continuous-time Laplace transforms and z -transforms, respectively. See Sect. 3.1.1.
4. The ROC of a unilateral Laplace transform of a time scale exponential, $e_\alpha(t)$, is a region external to two modified Hilger circles parameterized by α and the smallest and largest graininess of the time scale. See Theorem 3.2.
5. When a time scale has a constant asymptotic graininess, like \mathbb{Z} and \mathbb{R} , the ROC is external to a single modified Hilger circle. See Lemma 3.7.
6. Since $0 \leq \mu < \infty$, the Laplace transform of a time scale exponential, $e_\alpha(t)$, always converges to the right of a dimpled half-plane. See Lemma 3.5.
7. The ROCs for transcendental functions associated with the solution of linear time-invariant differential equations on time scales can be determined using the ROCs developed for the time scale exponential, $e_\alpha(t)$. See Sect. 4.
8. If the ROC of a time scale Laplace transform converges at a point, the ROC can be extrapolated to a larger region. The familiar cases of \mathbb{R} and \mathbb{Z} are special cases. See Sect. 5.

References

1. M. Bohner, A. Peterson, *Dynamic Equations on Time Scales: An Introduction with Applications* (Birkhäuser, Boston, 2001)
2. M. Bohner, A. Peterson (eds.), *Advances in Dynamic Equations on Time Scales* (Birkhäuser, Boston, 2002)
3. J.M. Davis, J. Henderson, K.R. Prasad, W.K.C. Yin, Solvability of a nonlinear second order conjugate eigenvalue problem on a time scale. *Abstr. Appl. Anal.* **5**, 91–99 (2000)
4. J.M. Davis, J. Henderson, K.R. Prasad, Upper and lower bounds for the solution of the general matrix Riccati differential equation on a time scale. *J. Comput. Appl. Math.* **141**, 133–145 (2002)
5. J.M. Davis, I.A. Gravagne, B.J. Jackson, R.J. Marks II, A.A. Ramos, The Laplace transform on time scales revisited. *J. Math. Anal. Appl.* **332**, 1291–1307 (2007)
6. I.A. Gravagne, J.M. Davis, J. Dacunha, R.J. Marks II, Bandwidth sharing for controller area networks using adaptive sampling, in *Proc. Int. Conf. Robotics and Automation (ICRA)*, New Orleans, LA, April 2004, pp. 5250–5255
7. G. Guseinov, Integration on time scales. *J. Math. Anal. Appl.* **285**(1), 107–127 (2003)
8. S. Hilger, Ein Masskettenkalkül mit Anwendung auf Zentrumsmannigfaltigkeiten. Ph.D. thesis, Universität Würzburg, Germany (1988)
9. S. Hilger, Special functions: Laplace and Fourier transform on measure chains. *Dyn. Syst. Appl.* **8**, 471–488 (1999)

10. R.J. Marks II, I. Gravagne, J.M. Davis, J.J. DaCunha, Nonregressivity in switched linear circuits and mechanical systems. *Math. Comput. Model.* **43**, 1383–1392 (2006)
11. R.J. Marks II, I.A. Gravagne, J.M. Davis, A generalized Fourier transform and convolution on time scales. *J. Math. Anal. Appl.* **340**(2), 901–919 (2008)
12. R.J. Marks II, *Handbook of Fourier Analysis and Its Applications* (Oxford University Press, London, 2009)
13. J. Seiffertt, S. Sanyal, D.C. Wunsch, Hamilton–Jacobi–Bellman equations and approximate dynamic programming on time scales. *IEEE Trans. Syst. Man Cybern. Part B* **38**(4), 918–923 (2008)
14. E. Talvila, The distributional Denjoy integral. *Real Anal. Exch.* **33**(1), 51–82 (2007/2008)